Journal of Nanostructure in Chemistry (2018) 8:23–32
https://doi.org/10.1007/s40097-017-0251-4

ORIGINAL RESEARCH

One-pot synthesis of S-doped Fe_2O_3/C magnetic nanocomposite as an adsorbent for anionic dye removal: equilibrium and kinetic studies

Hossein Khoshsang[1] · Ali Ghaffarinejad[1,2] · Hojjat Kazemi[3] · Yuan Wang[4] · Hamidreza Arandiyan[4]

Received: 4 November 2017 / Accepted: 8 December 2017 / Published online: 19 December 2017

Abstract

Novel S-doped Fe_2O_3/C nanocomposite was synthesized via a one-pot hydrothermal method and was used for the first time as an efficient adsorbent for Congo red dye (CR) removal from water solution. The obtained catalyst was characterized by various methods including Fourier transform infrared spectroscopy, energy dispersive X-ray spectrometry, vibration sample magnetometry, X-ray diffraction and field emission scanning electron microscopy. To improve the adsorption performance, some important parameters affecting dye removal were optimized such as adsorbent dosage, contact time, solution pH, initial dye concentration and ionic strength. At the optimum conditions, the maximum capacity of adsorption for this nanocomposite was 270.2 mg g^{-1}, which is better than other magnetic adsorbents for CR removal. The results of adsorption isotherm were matched with Langmuir model. Kinetic tests show that adsorption experimental data were best fitted by pseudo-first-order model.

Graphical abstract

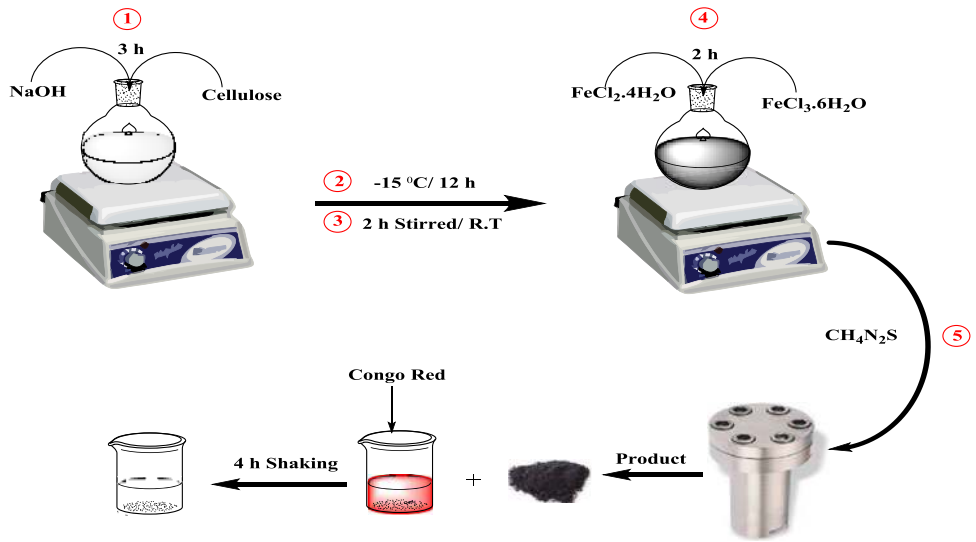

Keywords S-doped Fe_2O_3/C nanocomposite · Congo red · Adsorption · Magnetic separation · Kinetic study

✉ Ali Ghaffarinejad
Ghaffarinejad@iust.ac.ir

Extended author information available on the last page of the article

Introduction

Organic dyes are natural or synthetic compounds which have been widely applied in a number of processing industries such as leather, textile, cosmetics, packaging, food, and paper industries [1, 2]. There are more than 100,000 commercial dyes with an annual production of over 7×10^5 tons year^{-1} [3]. The extensive application of dyes in industries brings about big amount of toxic dyes and pigments waste discharging to the environment, which subsequently causes serious environmental problems and threat to human's health [4, 5]. The presence of organic dyes even in low concentrations has irreversible effects on human health from skin irritation, Heinz body formation, gastritis and tissue necrosis to the worst result of cancer [6]. Therefore, removing dye pollutants from the environment is an important and necessary task.

Congo red (CR), one of the important pollution dyes, is a sodium salt of benzidinediazobis-1-naphthylamine-4-sulfonic acid with chemical formula $C_{32}H_{22}N_6Na_2O_6S_2$ (Scheme 1). The presence of aromatic amine groups as toxic agent in water may endanger human and other living organisms [7, 8]. According to Merck® safety information, CR may cause cancer and possible risk of damage to the human fetus (Merck Material Safety Data Sheet) [9]. CR is highly soluble in water, has high resistance to the temperature and sunlight, and is stable against the biological and chemical degradation [10].

A number of methods have been reported to remove the dye pollutions from water, for example, filtration by membrane and nanomaterials, coagulation, photocatalytic decomposition, aerobic and anaerobic microbial degradation, flocculation, advanced oxidation processes and treatment with ozone [11, 12]. Among these methods, adsorption is the most convenient and promising strategy due to the easy operation, high efficiency, low energy requirement, and easy recovery or reuse of the adsorbent [10, 13]. Compared to other adsorbents for dye removal, magnetic materials possessed many advantages such as chemical stability, nontoxic synthesis, environmentally friendly, low cost and facile separation from the water solution [14, 15].

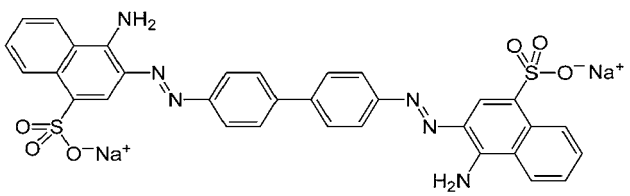

Scheme 1 The molecular structure of Congo red

Fe_2O_3 magnetic particles are frequently used as one of the suitable materials to remove the pollutants from environment For example, γ-Fe_2O_3 synthesized by metal etching approach was applied for the adsorption removal of methylene blue dye [16]. Activated carbon/α-Fe_2O_3 nanocomposite was prepared by simple pyrolysis route and utilized to degrade the acid yellow 17 dye from water [17]. In another work, S-doped α-Fe_2O_3 (α-Fe_2O_3/s) was synthesized with ferrous sulfate and $Na_2S_2O_3$ via a hybrid hydrothermal–calcination treatment for the photogeneration of acid orange 7 and phenol [18]. Similarly, γ-Fe_2O_3 and Fe_3O_4 nanoparticles loading on activated carbon were fabricated for the removal of cationic dye [19, 20] and Alizarin Red S [21]. Mesoporous carbon nanocomposite was synthesized via a facile impregnation–carbonization method for dye and heavy metal adsorption [22], and other carbon derivatives (carbon nanotubes and graphene) for heavy metal removal [23, 24]. In previous studies, Dutta and coworkers used γ-Fe_2O_3 nanoparticles for photodegradation of methylene blue and rose Bengal dye [25]. Wang et al. [26] used hydroxylated α-Fe_2O_3 for synergistic photocatalysis of Cr(VI) reduction and 4-chlorophenol degradation under visible light irradiation. Other reports about Fe_2O_3 magnetic composites for organic pollutant removal can be found in [27–31].

In this study, new magnetic nanocomposite S-doped Fe_2O_3/C was synthesized through a one-pot hydrothermal method. The preparation method was optimized by modifying several synthesis conditions and the physicochemical properties of prepared S-doped Fe_2O_3/C were studied by means of characterization methods. The synthesized S-doped Fe_2O_3/C was applied as an adsorbent for the first time for the removal of CR dye from water.

Experimental

Materials

Cellulose powder, thiourea, $FeCl_3 \cdot 6H_2O$, $FeCl_2 \cdot 4H_2O$, NaOH, HCl, and CR were purchased from Merck. All chemicals were of analytical grade applied without further purification. Deionized (DI) water was used to prepare all solutions.

Synthesis of S-doped Fe_2O_3/C nanocomposites

The typical preparation procedure of S-doped Fe_2O_3/C was depicted as follows: 8 g NaOH and 1.2 g cellulose powder were dissolved in 80 mL DI water. The mixture was stirred for 3 h at room temperature and aged at − 15 °C for 12 h. After that, the mixture was stirred vigorously by a magnet stirrer at room temperature for 2 h to dissolve cellulose. 0.28 g $FeCl_3 \cdot 6H_2O$ and 0.15 g $FeCl_2 \cdot 4H_2O$ were then added

to the solution simultaneously and stirred for 2 h. Afterward, 1 g thiourea was added to the mixture and stirred for a few minutes before transferring the mixture to a Teflon sealed autoclave at 160 °C for 10 h. After cooling to room temperature, S-doped Fe_2O_3/C nanocomposite was collected by a magnet and washed for several times with DI water and diluted HCl. The product was finally obtained after drying in a vacuum oven at 60 °C for 12 h.

Characterization

The properties of the S-doped Fe_2O_3/C nanocomposite were determined by different techniques. Morphology of adsorbent was studied by FE-SEM model of TESCAN, Mira III LMU, the Czech Republic at 15 kV. FT-IR analysis was conducted by Shimadzu FTIR 8400S spectrophotometer (Japan). Field emission scanning electron microscopy with energy dispersive X-ray spectroscopy (FE-SEM/EDS, TESCAN, Mira II LMU, Czech Republic) was used for the elemental analysis. XRD pattern was obtained in 2θ between 10 and 80° with a Philips-pw 1800 diffractometer, which was equipped with Cu-Kα irradiation ($\lambda = 0.1524$ nm) source. Magnetic property was measured by VSM analysis (Lake Shore 7410, USA). UV–Vis spectra were obtained with a Shimadzu UV–Visible Spectrophotometer model UV-mini 1240 (Japan).

Results and discussion

FE-SEM images and EDS elemental analysis of S-doped Fe_2O_3/C nanocomposite

Figure 1 shows SEM images of S-doped Fe_2O_3/C nanocomposite. It can be seen that Fe_2O_3 nanoparticles are decorated on the carbon surface and the estimated mean particle size of Fe_2O_3 is about 20 nm (Fig. 1c). EDS spectrum of S-doped Fe_2O_3/C is presented in Fig. 1d. The peaks related to Fe, C, O and S elements are obviously observed, suggesting the successful synthesis of the S-doped Fe_2O_3/C nanocomposite.

FT-IR studies

The formation of S-doped Fe_2O_3/C was further confirmed by FT-IR spectroscopy as shown in Fig. 2, which indicates the spectra of cellulose powder and S-doped Fe_2O_3/C. The stretching vibration band at 3434 cm^{-1} can be correlated with hydroxyl groups (OH) adsorbed on the surface. The bands between 1000 and 1400 cm^{-1} can be assigned to the C–OH stretching and O–H bending vibrations. The bands attributed to Fe–O and C–S stretching at around 577 cm^{-1} is only observed in S-doped Fe_2O_3/C spectrum. The FT-IR results are well matched with the spectra of previous research.

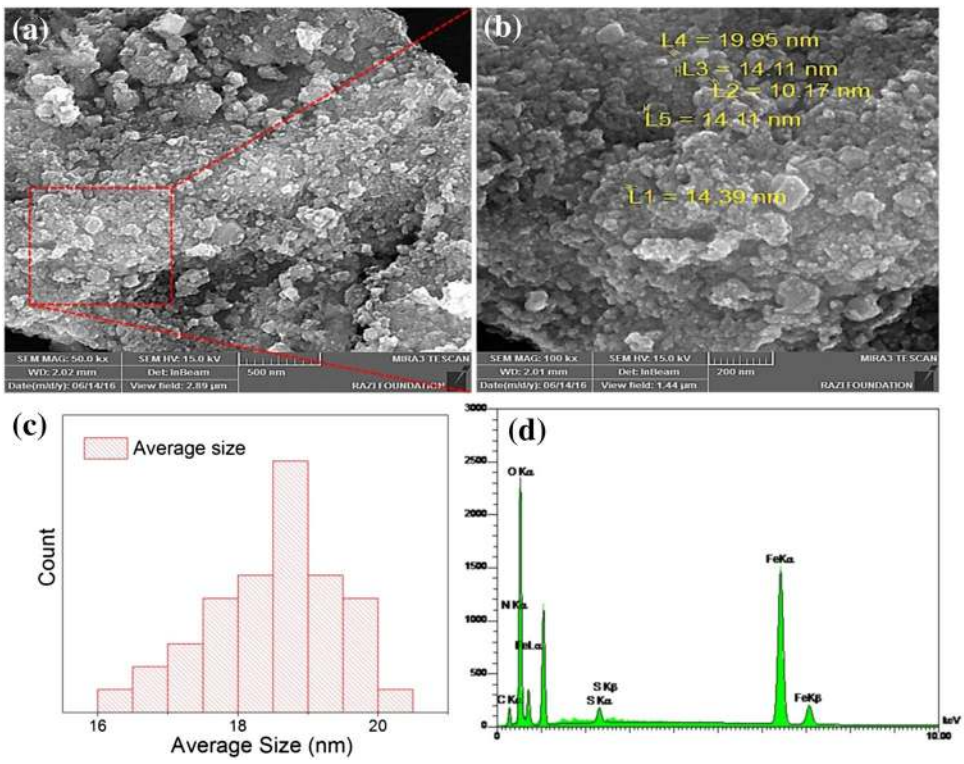

Fig. 1 FE-SEM images of S-doped Fe_2O_3/C nanocomposite with two magnifications **a** ×50 K, **b** ×100 K, **c** average size distribution and **d** EDS elemental maps of the sample

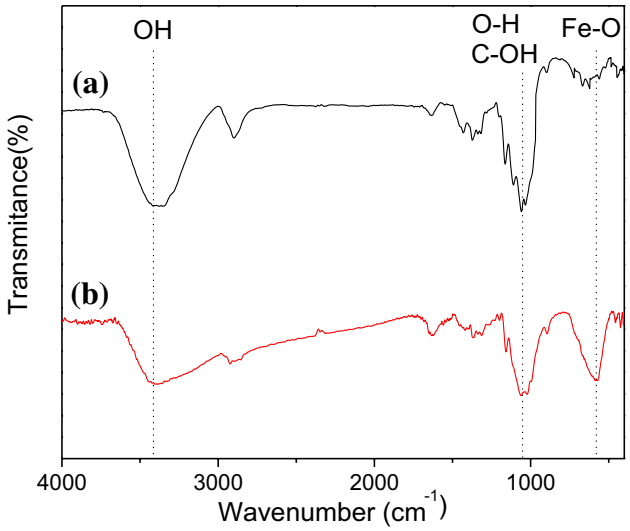

Fig. 2 FT-IR spectra of **a** cellulose powder **b** S-doped Fe_2O_3/C nanocomposite

XRD study

X-ray diffraction patterns of the S-doped Fe_2O_3/C nanocomposite are shown in Fig. 3. Compared to the standard JCPDS Card No. 01-79-0007 of hematite α-Fe_2O_3, the main diffraction peaks at $2\theta = 24.18$, 33.19, 35.68, 40.91, 49.52, 54.13, 64.10 and 72.03° are assigned to (012), (104), (110), (113), (024), (116), (300) and (101) planes, respectively. It is found that the diffraction peaks at $2\theta = 30.24$, 35.63, 43.28, 57.27 and 62.92° are related to (220), (311), (400), (511) and (440), respectively, in standard maghemite γ-Fe_2O_3 according to 00-39-1346 reference pattern. The result shows that no diffraction peaks for crystalline carbon are detected, which may be due to the formation of amorphous carbon structure [32].

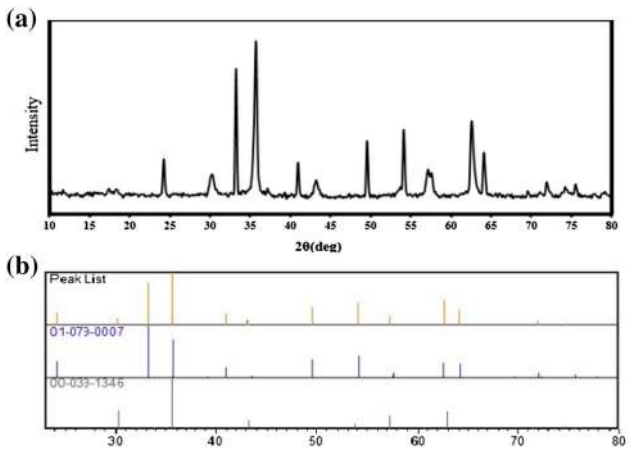

Fig. 3 **a** X-ray diffraction pattern of S-doped Fe_2O_3/C nanocomposite, **b** comparison between S-doped Fe_2O_3/C and Fe_2O_3 (α and γ) reference patterns

Average particle diameter (D) of different nanoparticles was calculated from the main peaks using Scherrer equation (Eq. 1):

$$D = \frac{k\lambda}{B\cos(\theta)} \quad (1)$$

where D is crystallite size in nm; k is a quantity without dimension, the so-called shape factor, which usually takes a value of about 0.9; λ is the wavelength of X-ray tube in nm; β is peak board at half maximum height (FWHM), its unit must be in radians, and θ is the Bragg angle in degree. The nanoparticle size determined with this equation for α-Fe_2O_3 and γ-Fe_2O_3 is about 38.03 and 23.8 nm, respectively.

Magnetic property

Figure 4 gives the magnetic hysteresis loops of S-doped Fe_2O_3/C nanocomposite at room temperature. The saturation magnetization is found to be 39.33 emu g^{-1} for the proposed nanocomposite. The decrease in saturation magnetization value for this nanocomposite is due to the presence of non-magnetic carbon and α-Fe_2O_3 (Hematite). However, the VSM curve indicates that S-doped Fe_2O_3/C nanocomposite exhibited enough magnetic properties to be separated from the water solution by a magnet.

CR dye removal studies

In this work, to obtain the best conditions, some important parameters affecting dye removal were studied. The concentration of CR dye was measured by a UV–Vis spectrophotometer at $\lambda_{max} = 498$ nm. The following formula specifies the percentage of dye removal:

$$\text{Removal}(\%) = \frac{(C_0 - C_e)}{C_0} \times 100 \quad (2)$$

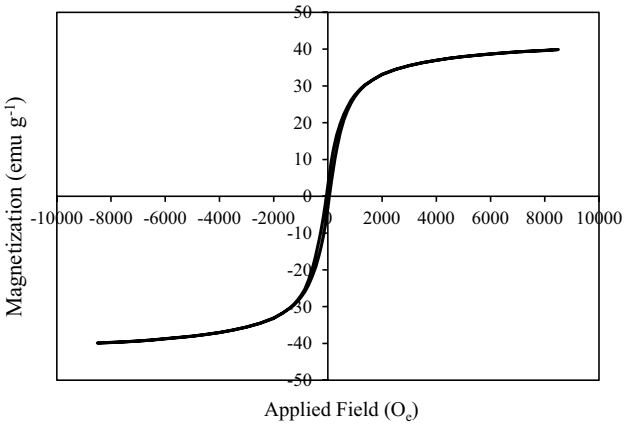

Fig. 4 Magnetic hysteresis loops of the S-doped Fe_2O_3/C nanocomposite

where C_e and C_0 are the equilibrium and initial dye concentrations (mg L^{-1}), respectively. The amount of dye adsorbed on adsorbent at during time t (q_t, mg g^{-1}) was calculated according to Eq. 3:

$$q_t = \frac{(C_0 - C_t)V}{W} \quad (3)$$

where V is the solution volume (L) and W is the adsorbent weight (g).

Effect of adsorbent dosage

The adsorption dosage is an important parameter for dye removal. In the economic view, the researchers are perusing optimal adsorption capacity with the minimum usage of adsorbent dosage [33]. For this study, various amounts of S-doped Fe_2O_3/C nanocomposite (3, 4, 5, 10 and 15 mg) were added to 40 mL of 10 mg L^{-1} CR dye solution at pH 5 with 200 rpm shaking speed for 300 min. Figure 5 shows the changes of q_e and dye removal (%) vs. adsorbent dosage. Along with the increase of adsorbent dosage from 3 to 5 mg, both q_e and dye removal percentage show drastically improvement. However, as the amount of adsorbent increase to 10 and 15 mg, the variation trend exhibits a slow growth, suggesting the saturation of dye with 5 mg absorbent. Thus, 5 mg of adsorbent was determined as the most effective amount and higher dosages led to significant decrease in adsorption capacity.

Effect of solution pH on CR dye adsorption

pH value in the solution is another important parameter affecting the dye removal efficiency. The influence of initial pH for CR adsorption on the S-doped Fe_2O_3/C nanocomposite is illustrated in Fig. 6. In this study, 5 mg adsorbent (optimum amount obtained from above experiment) was added to 40 mL of 10 mg L^{-1} CR solution at the pH range of 5–10 (pH was adjusted with 0.1 M HCl or 0.1 M NaOH solutions). According to Fig. 6, the best result in this pH range is at pH 5. The possible reason for this result is the anionic structure of CR dye which causes repulse of adsorbent at higher pH values. In the acidic environment, the adsorbent has neutral or positive charge, which attracts more CR molecules with a negative charge, resulting in the improvement of adsorption process.

Effect of shaking time

The effect of contact time on adsorption of CR by S-doped Fe_2O_3/C nanocomposite at optimum pH and adsorbent dosage was examined and the results of this study are presented in Fig. 7. The results show that the adsorption capacity and percent of dye adsorption increase rapidly at the initial increasing period of contact time duration, but slow down after 150 min and reach almost equilibrium at about 250 min. Hence, the equilibrium time for dye and adsorbent contact is optimized as 250 min.

Effect of initial dye concentration

The adsorption capacity for dye removal is highly related to the initial dye concentration. In present study, the effect of concentrations of dye (10−100 mg L^{-1}) on the removal performance was investigated at the optimum dosage, pH and shaking time. As shown in Fig. 8 the dye removal percentage decreases along with the increase of the initial

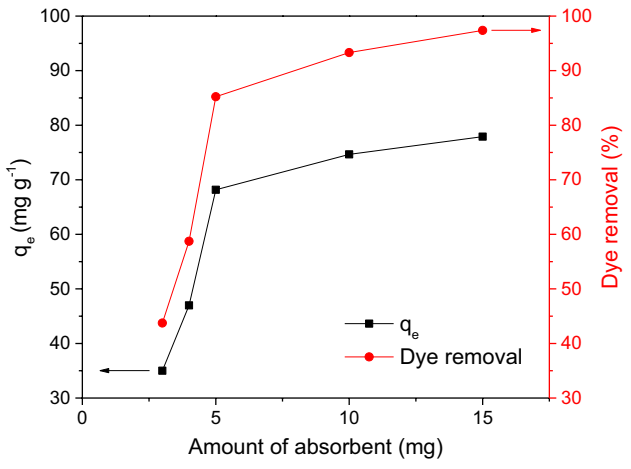

Fig. 5 Effect of S-doped Fe_2O_3/C dosage on adsorption of CR dye (C_0 = 10 mg L^{-1}, initial solution pH = 5, shaker speed = 200 rpm, CR solution volume = 40 mL)

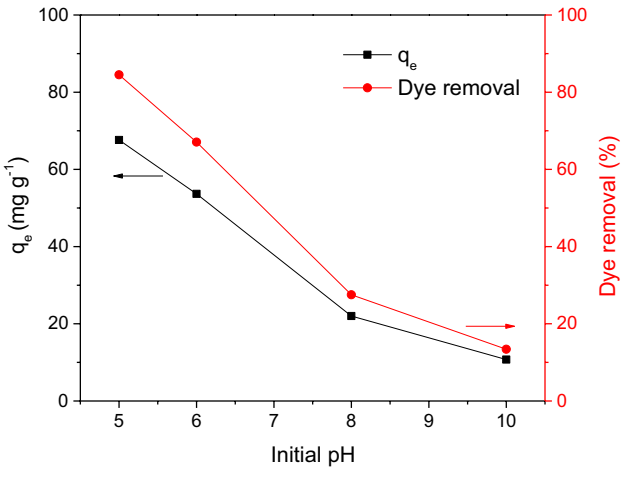

Fig. 6 The effect of pH value on CR removal efficiency by the magnetic adsorbent (C_0 = 10 mg L^{-1}, adsorbent dosage = 5 mg, solution volume = 40 mL, shaker speed = 200 rpm)

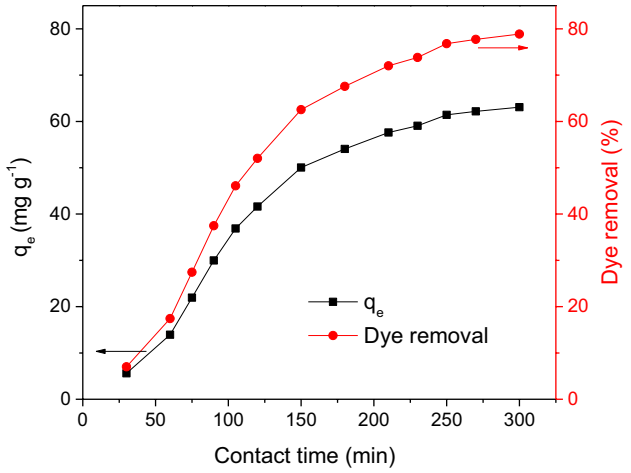

Fig. 7 Effect of shaking time on adsorption of CR dye (C_0 = 10 mg L^{-1}, CR solution volume = 40 mL, adsorbent dosage = 5 mg, shaker speed = 200 rpm, pH = 5)

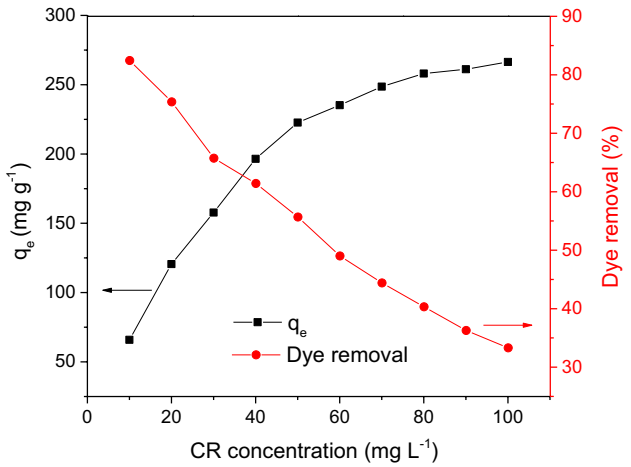

Fig. 8 Effect of initial dye concentration on removal of CR (CR solution volume = 40 mL, adsorbent dosage = 5 mg, shaker speed = 200 rpm, pH = 5)

dye concentration which is because of the saturation of adsorption sites on the magnetic adsorbent surface. Also, by increasing the initial dye concentration, the capacity of adsorbent increases, which may be due to the high driving force for mass transfer at a high initial dye concentration.

Influence of ionic strength on adsorption efficiency

To investigate the ionic strength on adsorption efficiency, 0.01 mol L^{-1} of NaCl, Na_2CO_3 and $NaHCO_3$ were added to 40 mL of 10 mg L^{-1} CR solution (pH = 5) containing 5 mg adsorbent (Fig. 9). In the presence of Cl^-, CO_3^{2-} and HCO_3^-, the adsorption efficiency of CR dye decreases to about 12.5, 29.8 and 27.5%, respectively. It indicates that a

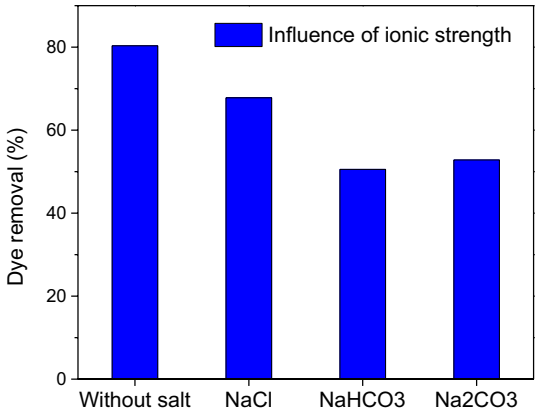

Fig. 9 Influence of ionic strength for various salts on CR adsorption (C_0 = 10 mg L^{-1}, solution volume = 40 mL, adsorbent dosage = 5 mg, shaker speed = 200 rpm, pH = 5)

competitive adsorption occurs between the anionic CR dye molecules and the anions present in the salt solution.

Adsorption isotherm

To determine the adsorption behavior of CR on S-doped Fe_2O_3/C nanocomposite, three important isotherm models (Langmuir, Freundlich and Temkin) were used. The Langmuir model assumes that the process of adsorption on adsorbent is monolayer and homogeneous, and there is no interaction between the adsorbent and dye molecules. The equation of Langmuir isotherm is shown as follows:

$$\frac{1}{q_e} = \frac{1}{q_m} + \frac{1}{bq_mC_e} \tag{4}$$

where C_e (mg L^{-1}) is equilibrium concentration of CR in solution; q_e (mg g^{-1}) is adsorption capacity of CR adsorbed on S-doped Fe_2O_3/C nanocomposites at equilibrium; q_m (mg g^{-1}) is theoretical maximum adsorption for CR on S-doped Fe_2O_3/C nanocomposites; b (L mg^{-1}) is a Langmuir constant that is related to the heat of adsorption [34, 35].

$$R_l = \frac{1}{1 + R_lC_0} \tag{5}$$

In Eq. (5), R_L gives important information about the nature of dye adsorption, where K_L is the Langmuir constant (L mg^{-1}) and C_0 (mg L^{-1}) is the initial dye concentration. The value of R_L indicates the adsorption nature, if $R_L > 1$, $R_L = 1$, $0 < R_L < 1$ or $R_L = 0$, it will be unfavorable (desorption occurs in during the adsorption process), linear (isotherm is totally a straight line), favorable (process adsorption occurs normally under conditions tested), and irreversible (adsorption is still too strong), respectively. R_L values of CR adsorption on to S-doped

Table 1 Adsorption isotherm constants for adsorption of CR on S-doped Fe_2O_3/C

Langmuir	
q_e	270.2
b	0.178
R_L	0.059–0.358
R^2	0.992
Freundlich	
K_F	62.445
n	2.668
R^2	0.954
Temkin	
K_T	1.748
b_T	42.150
R^2	0.989

Fe_2O_3/C nanocomposite were calculated and these values were between 0 and 1 at different concentrations (minimum $R_L = 0.059$ and maximum $R_L = 0.358$), indicating favorable adsorption onto adsorbent (Table 1) [36].

In the Freundlich isotherm, a heterogeneous surface and a multilayer adsorption on the adsorbent surface are assumed. The mathematical model can be written by the following equation:

$$\ln q_e = \ln K_f + \frac{1}{n}\ln C_e \quad (6)$$

where K_f and n are constant incorporating all factors affecting the adsorption process such as adsorption capacity and intensity. If $n = 1$, the adsorption is linear; if $n < 1$, chemical adsorption process occurs; if $n > 1$, adsorption process is physical. Therefore, adsorption of CR dye on magnetic nanocomposite was a physical and heterogeneous process and is a beneficial adsorption (Table 1) [37, 38]. In the Temkin model, adsorbent–adsorbent interaction is considered and presented by Eq. 7:

$$q_e = B\ln A + B\ln C_e \quad (7)$$

In this equation, A is a constant for equilibrium binding (L mg^{-1}) in accordance with maximum binding energy and constant B ($B = RT/b$) is the Temkin isotherm energy that is related to the heat of adsorption. R is the universal gas constant (8.314 J mol^{-1} K^{-1}), T is the absolute temperature (K), and b is a constant [39]. The results were fitted with these isotherms (Fig. 10), which the best fit was obtained for Langmuir model ($R^2 = 0.992$). Therefore, according to this isotherm the adsorption phenomenon is monolayer and homogeneous on the magnetic adsorbent. The results of adsorption isotherm constants for adsorption of CR on to the S-doped Fe_2O_3/C are presented in Table 1.

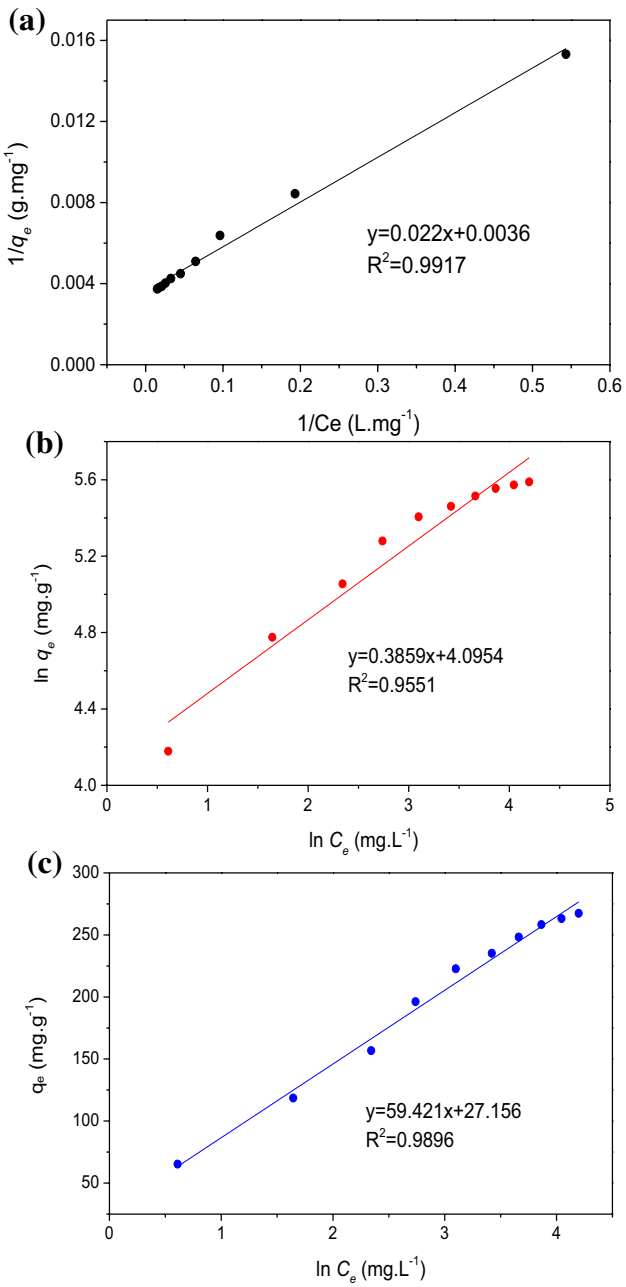

Fig. 10 **a** Langmuir, **b** Freundlich and **c** Temkin adsorption isotherms for the adsorption of the CR on to S-doped Fe_2O_3/C at 298 K

Dye adsorption kinetic study

The kinetics of dye adsorption onto adsorbent can be used to locate the best operating conditions for the adsorption process [33]. For kinetic studies, pseudo-first-order and pseudo-second-order are two commonly used models to determine the factors that affect the rate of absorption. The first adopted method is a Lagergren pseudo-first-order [40], which is used widely and expressed by the Eq. 8:

$$\ln\left(q_e - q_t\right) = \ln q_e - \frac{k_1 t}{2.303} \quad (8)$$

In this equation k_1 (min^{-1}) is the rate constant for pseudo-first (Lagergren) order, q_t (mg g^{-1}) and q_e (mg g^{-1}) are adsorption capacities at time t (min) and the equilibrium condition, respectively. The values of the constants k_1 and q_e were obtained from the linear plot of ln (q_e–q_t) vs. t.

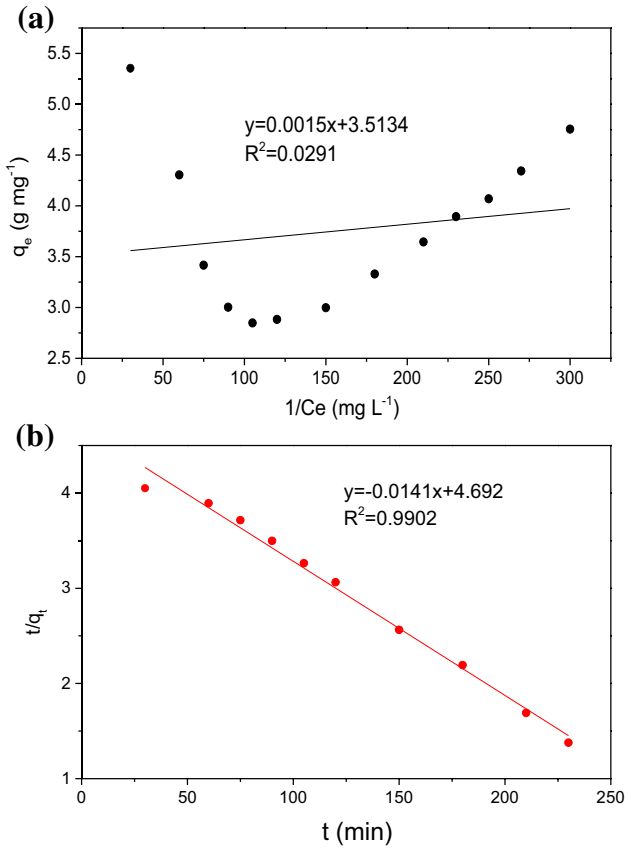

Fig. 11 **a** Pseudo-first-order and **b** pseudo-second-order plots for the adsorption of CR dye on to S-doped Fe_2O_3/C

The simplified Lagergren pseudo-second-order model of dye adsorption described as:

$$\frac{t}{q_t} = \frac{1}{k_2 q_e^2} + \frac{t}{q_e} \quad (9)$$

where k_2 is the pseudo-second-order rate constant (g mg^{-1} min^{-1}) [41]. The experimental data were plotted according to both pseudo-first- ($R^2 = 0.990$) and pseudo-second-order ($R^2 = 0.029$) models (Fig. 11), which the best linear relation was observed with the rate constant of 0.032 min^{-1} for pseudo-first-order kinetic.

Table 2 compares q_{max} of the proposed S-doped Fe_2O_3/C nanocomposite with some magnetic adsorbents which have been reported recently for CR dye removal. This comparison results indicate that the proposed magnetic nanocomposite has comparable q_{max} with other reported adsorbents.

Conclusion

In summary, a novel adsorbent magnetically separable S-doped Fe_2O_3/C nanocomposite was prepared by a simple one-pot hydrothermal method. Nanocomposite properties were determined by FE-SEM, XRD, FT-IR, EDS and VSM methods and the removal performance of the CR dye from water solution was determined on the obtained materials. The effect of important parameters on dye removal performance including initial solution pH, adsorbent dosage, shaking time, initial dye concentration with ionic strength was optimized. The adsorption data were fitted well with the Langmuir isotherm and the kinetic results were well matched with the pseudo-first-order model. Owing to the low cost, ease of preparation and high adsorption capacity, the investigated magnetic nanocomposite can be a suitable adsorbent for anionic dye removal.

Acknowledgements The authors gratefully acknowledge the Iran University of Science and Technology for supporting this research.

Table 2 Comparison of q_{max} for different magnetic adsorbents for removal of CR

Adsorbent	q_{max} (mg g^{-1})	References
CTAB-coated Fe_3O_4 NPs	93.46	[42]
CABI nanogoethite	181.1	[43]
α-Fe_2O_3	313.6	[24]
γ-Fe_2O_3	208.3	[44]
$NiFe_2O_4$/ZnO	221.7	[45]
Fe_3O_4/MgAl-layered double hydroxide composite	253	[46]
pTSAPani@GO-CNT nanocomposite	66.66	[47]
Silica coated Fe_3O_4 magnetic nanospheres	54.65	[48]
Magnetic$Sr_{5x}Ba_{3x}(PO_4)_3(OH)/Fe_3O_4$ nanopowder	417	[49]
S-doped Fe_2O_3/C	270.2	Present study

References

1. Seow, T.W., Lim, C.K.: Removal of dye by adsorption: a review. Int. J. Appl. Eng. Res. **11**, 2675–2679 (2016)
2. Pal, J., Deb, M.K.: Efficient adsorption of congo red dye from aqueous solution using green synthesized coinage nanoparticles coated activated carbon beads. Appl. Nanosci. **4**, 967–978 (2014)
3. Li, Q., Xue, D.X., Zhang, Y.F., Zhang, Z.H., Wang, Q., Gao, Z., Bai, J.: A copper-organic framework as scavenger towards organic dyes pollutants via physical adsorption and visible-light photodegradation. Inorg. Chem. Commun. **85**, 78–83 (2017)
4. Pereira, L., Alves, M.: Dyes—environmental impact and remediation, in environmental protection strategies for sustainable development. In: Malik, A., Grohmann, E. (eds.) pp. 111–162. Springer Netherlands: Dordrecht (2012)
5. Zahir, A., Aslam, Z., Kamal, M.S., Ahmad, W., Abbas, A., Shawabkeh, R.A.: Development of novel cross-linked chitosan for the removal of anionic Congo red dye. J. Mol. Liq. **244**, 211–218 (2017)
6. Abdellaoui, K., Pavlovic, I., Bouhent, M., Benhamou, A., Barriga, C.: A comparative study of the amaranth azo dye adsorption/desorption from aqueous solutions by layered double hydroxides. Appl. Clay Sci. **143**, 142–150 (2017)
7. Liu, X., Li, W., Chen, N., Xing, X., Dong, C., Wang, Y.: Ag–ZnO heterostructure nanoparticles with plasmon-enhanced catalytic degradation for Congo red under visible light. RSC Adv. **5**, 34456–34465 (2015)
8. Gharehbaghi, M., Shemirani, F.: A novel method for dye removal: ionic liquid-based dispersive liquid-liquid extraction (IL-DLLE). CLEAN–Soil Air Water **40**, 290–297 (2012)
9. Congo red (CI 22120) CAS 573-58-0 | 101340—Merck Millipore. http://www.merckmillipore.com/INTL/en/product/Congo-red-C.I.-22120,MDA_CHEM-101340. Accessed 26 Nov 2017
10. Lei, C., Pi, M., Jiang, C., Cheng, B., Yu, J.: Synthesis of hierarchical porous zinc oxide (ZnO) microspheres with highly efficient adsorption of Congo red. J. Colloid Interface Sci. **490**, 242–251 (2017)
11. Rahimi, R., Kerdari, H., Rabbani, M., Shafiee, M.: Synthesis, characterization and adsorbing properties of hollow Zn-Fe_2O_4 nanospheres on removal of Congo red from aqueous solution. Desalination **280**, 412–418 (2011)
12. Torabinejad, A., Nasirizadeh, N., Yazdanshenas, M.E., Tayebi, H.A.: Synthesis of conductive polymer-coated mesoporous MCM-41 for textile dye removal from aqueous media. J. Nanostruct. Chem. **7**, 217–229 (2017)
13. Saroyan, H.S., Giannakoudakis, D.A., Sarafidis, C.S., Lazaridis, N.K., Deliyanni, E.A.: Effective impregnation for the preparation of magnetic mesoporous carbon: application to dye adsorption. J. Chem. Technol. Biotechnol. **92**, 1899–1911 (2017)
14. Bagheri, A.R., Ghaedi, M., Asfaram, A., Bazrafshan, A.A., Jannesar, R.: Comparative study on ultrasonic assisted adsorption of dyes from single system onto Fe_3O_4 magnetite nanoparticles loaded on activated carbon: experimental design methodology. Ultrason. Sonochem. **34**, 294–304 (2017)
15. Liu, Y., Chen, L., Yang, Y., Li, M., Li, Y., Dong, Y.: The efficient removal of Cu (II) from aqueous solutions by Fe_3O_4@hexadecyl trimethoxysilane@chitosan composites. J. Mol. Liq. **219**, 341–349 (2016)
16. Zhang, L.Y., Zhang, W., Zhou, Z., Li, C.M.: γ-Fe_2O_3 nanocrystals-anchored macro/meso-porous graphene as a highly efficient adsorbent toward removal of methylene blue. J. Colloid Interface Sci. **476**, 200–205 (2016)
17. Ranjithkumar, V., Sangeetha, S., Vairam, S.: Synthesis of magnetic activated carbon/α-Fe_2O_3 nanocomposite and its application in the removal of acid yellow 17 dye from water. J. Hazard. Mater. **273**, 127–135 (2014)
18. Guo, L., Chen, F., Fan, X., Cai, W., Zhang, J.: S-doped α-Fe_2O_3 as a highly active heterogeneous Fenton-like catalyst towards the degradation of acid orange 7 and phenol. Appl. Catal. B. **96**, 162–168 (2010)
19. Asfaram, A., Ghaedi, M., Hajati, S., Goudarzi, A.: Synthesis of magnetic γ-Fe_2O_3-based nanomaterial for ultrasonic assisted dyes adsorption: modeling and optimization. Ultrason. Sonochem. **32**, 418–431 (2016)
20. Altıntıg, E., Altundag, H., Tuzen, M., Sarı, A.: Effective removal of methylene blue from aqueous solutions using magnetic loaded activated carbon as novel adsorbent. Chem. Eng. Res. Des. **122**, 151–163 (2017)
21. Fayazi, M., Ghanei-Motlagh, M., Taher, M.A.: The adsorption of basic dye (Alizarin red S) from aqueous solution onto activated carbon/γ-Fe_2O_3 nano-composite: kinetic and equilibrium studies. Mater. Sci. Semicond. Process. **40**, 35–43 (2015)
22. Chen, L., Ji, T., Mu, L., Shi, Y., Brisbin, L., Guo, Z., Khan, M.A., Young, D.P., Zhu, J.: Facile synthesis of mesoporous carbon nanocomposites from natural biomass for efficient dye adsorption and selective heavy metal removal. RSC Adv. **6**, 2259–2269 (2016)
23. Yu, G., Lu, Y., Guo, J., Patel, M., Bafana, A., Wang, X., Qiu, B., Jeffryes, C., Wei, S., Guo, Z., Wujcik, E.K.: Carbon nanotubes, graphene, and their derivatives for heavy metal removal. Adv. Compos. Hybrid Mater. (2017). 10.1007/s42114-017-0004-3
24. Satheesh, R., Vignesh, K., Rajarajan, M., Suganthi, A., Sreekantan, S., Kang, M., Kwak, B.S.: Removal of congo red from water using quercetin modified α-Fe_2O_3 nanoparticles as effective nanoadsorbent. Mater. Chem. Phys. **180**, 53–65 (2016)
25. Dutta, A.K., Maji, S.K., Adhikary, B.: γ-Fe_2O_3 nanoparticles: an easily recoverable effective photo-catalyst for the degradation of rose bengal and methylene blue dyes in the waste-water treatment plant. Mater. Res. Bull. **49**, 28–34 (2014)
26. Wang, J.C., Ren, J., Yao, H.C., Zhang, L., Wang, J.S., Zang, S.Q., Zang, L., Han, F., Li, Z.J.: Synergistic photocatalysis of Cr(VI) reduction and 4-chlorophenol degradation over hydroxylated α-Fe_2O_3 under visible light irradiation. J. Hazard. Mater. **311**, 11–19 (2016)
27. Liu, Y., Jin, W., Zhao, Y., Zhang, G., Zhang, W.: Enhanced catalytic degradation of methylene blue by α-Fe_2O_3/graphene oxide via heterogeneous photo-Fenton reactions. Appl. Catal. B. **206**, 642–652 (2017)
28. Zhu, H.Y., Jiang, R., Xiao, L.: Adsorption of an anionic azo dye by chitosan/kaolin/γ-Fe_2O_3 composites. Appl. Clay Sci. **48**, 522–526 (2010)
29. Chen, H., Li, T., Zhang, L., Wang, R., Jiang, F., Chen, J.: Pb(II) adsorption on magnetic γ-Fe_2O_3/titanate nanotubes composite. J. Environ. Chem. Eng. **3**, 2022–2030 (2015)
30. Saiphaneendra, B., Saxena, T., Singh, S.A., Madras, G., Srivastava, C.: Synergistic effect of co-existence of hematite (α-Fe_2O_3) and magnetite (Fe_3O_4) nanoparticles on graphene sheet for dye adsorption. J. Environ. Chem. Eng. **5**, 26–37 (2017)
31. Wang, Q., Zhu, N., Liu, E., Zhang, C., Crittenden, J.C., Zhang, Y., Cong, Y.: Fabrication of visible-light active Fe_2O_3-GQDs/NF-TiO_2 composite film with highly enhanced photoelectrocatalytic performance. Appl. Catal. B. **205**, 347–356 (2017)

32. Zhang, Z., Kong, J.: Novel magnetic Fe_3O_4@C nanoparticles as adsorbents for removal of organic dyes from aqueous solution. J. Hazard. Mater. **193**, 325–329 (2011)
33. Yagub, M.T., Sen, T.K., Afroze, S., Ang, H.M.: Dye and its removal from aqueous solution by adsorption: a review. Adv. Colloid Interface Sci. **209**, 172–184 (2014)
34. Jia, X.J., Wang, J., Wu, J., Du, Y., Zhao, B., den Engelsen, D.: Bouquet-like calcium sulfate dihydrate: a highly efficient adsorbent for Congo red dye. RSC Adv. **5**, 72321–72330 (2015)
35. Langmuir, I.: The constitution and fundamental properties of solids and liquids. Part I. Solids. J. Am. Chem. Soc. **38**, 2221–2295 (1916)
36. Wibowo, E., Rokhmat, M., Abdullah, M.: Reduction of seawater salinity by natural zeolite (Clinoptilolite): adsorption isotherms, thermodynamics and kinetics. Desalination **409**, 146–156 (2017)
37. Erentürk, S., Malkoç, E.: Removal of lead (II) by adsorption onto *Viscum album* L.: effect of temperature and equilibrium isotherm analyses. Appl. Surf. Sci. **253**, 4727–4733 (2007)
38. Freundlich, H.: Over the adsorption in solution. J. Phys. Chem. **57**, e470 (1906)
39. Tempkin, M., Pyzhev, V.: Kinetics of ammonia synthesis on promoted iron catalyst. Acta Phys. Chim. USSR. **12**, 327 (1940)
40. Miandad, R., Kumar, R., Barakat, M.A., Basheer, C., Aburiazaiza, A.S., Nizami, A.S., Rehan, M.: Untapped conversion of plastic waste char into carbon-metal LDOs for the adsorption of Congo red. J. Colloid Interface Sci. **511**, 402–410 (2018)
41. Abdi, J., Vossoughi, M., Mahmoodi, N.M., Alemzadeh, I.: Synthesis of metal-organic framework hybrid nanocomposites based on GO and CNT with high adsorption capacity for dye removal. Chem. Eng. J. **326**, 1145–1158 (2017)
42. Saksornchai, E., Kavinchan, J., Thongtem, S., Thongtem, T.: Simple wet-chemical synthesis of superparamagnetic CTAB-modified magnetite nanoparticles using as adsorbents for anionic dye Congo red removal. Mater. Lett. **213**, 138–142 (2018)
43. Munagapati, V.S., Kim, D.S.: Equilibrium isotherms, kinetics, and thermodynamics studies for congo red adsorption using calcium alginate beads impregnated with nano-goethite. Ecotoxicol. Environ. Safe. **141**, 226–234 (2017)
44. Afkhami, A., Moosavi, R.: Adsorptive removal of Congo red, a carcinogenic textile dye, from aqueous solutions by maghemite nanoparticles. J. Hazard. Mater. **174**, 398–403 (2010)
45. Zhu, H.Y., Jiang, R., Fu, Y.Q., Li, R.R., Yao, J., Jiang, S.T.: Novel multifunctional $NiFe_2O_4$/ZnO hybrids for dye removal by adsorption, photocatalysis and magnetic separation. Appl. Surf. Sci. **369**, 1–10 (2016)
46. Shan, R.R., Yan, L.G., Yang, K., Yu, S.J., Hao, Y.F., Yu, H.Q., Hao, Y.F., Yoa, H.-Q., Du, B.: Magnetic Fe_3O_4/MgAl-LDH composite for effective removal of three red dyes from aqueous solution. Chem. Eng. J. **252**, 38–46 (2014)
47. Ansari, M.O., Kumar, R., Ansari, S.A., Ansari, S.P., Barakat, M.A., Alshahrie, A., Cho, M.H.: Anion selective pTSA doped polyaniline@graphene oxide-multiwalled carbon nanotube composite for Cr(VI) and Congo red adsorption. J. Colloid Interface Sci. **496**, 407–415 (2017)
48. Wang, P., Wang, X., Yu, S., Zou, Y., Wang, J., Chen, Z., Alharbi, N.S., Alsaedi, A., Hayat, T., Chen, Y., Wang, X.: Silica coated Fe_3O_4 magnetic nanospheres for high removal of organic pollutants from wastewater. Chem. Eng. J. **306**, 280–288 (2016)
49. Zhang, F., Ma, B., Jiang, X., Ji, Y.: Dual function magnetic hydroxyapatite nanopowder for removal of malachite green and Congo red from aqueous solution. Powder Technol. **302**, 207–214 (2016)

Affiliations

Hossein Khoshsang[1] · Ali Ghaffarinejad[1,2] · Hojjat Kazemi[3] · Yuan Wang[4] · Hamidreza Arandiyan[4]

[1] Research Laboratory of Real Samples Analysis, Faculty of Chemistry, Iran University of Science and Technology, Tehran 1684613114, Iran

[2] Electroanalytical Chemistry Research Center, Iran University of Science and Technology, Tehran 1684613114, Iran

[3] Research Institute of Petroleum Industry, Tehran 1485733111, Iran

[4] Particles and Catalysis Research Group, School of Chemical Engineering, The University of New South Wales, Sydney, NSW 2052, Australia